Synthesis of a Modified $PC_{70}BM$ and Its Application as an Electron Acceptor with Poly(3-hexylthiophene) as an Electron Donor for Efficient Bulk Heterojunction Solar Cells

Surya Prakash Singh CH. Pavan Kumar, G. D. Sharma,* Rajnish Kurchania, and M. S. Roy*

A simple and effective modification of phenyl-C_{70}-butyric acid methyl ester ($PC_{70}BM$) is carried out in a single step after which the material is used as electron acceptor for bulk heterojunction polymer solar cells (PSCs). The modified $PC_{70}BM$, namely CN-$PC_{70}BM$, showed broader and stronger absorption in the visible region (350–550 nm) of the solar spectrum than $PC_{70}BM$ because of the presence of a cyanovinylene 4-nitrophenyl segment. The lowest unoccupied molecular energy level (LUMO) of CN-$PC_{70}BM$ is higher than that of $PC_{70}BM$ by 0.15 eV. The PSC based on the blend (cast from tetrahydrofuran (THF) solution) consists of P3HT as the electron donor and CN-$PC_{70}BM$ as the electron acceptor and shows a power conversion efficiency (PCE) of 4.88%, which is higher than that of devices based on $PC_{70}BM$ as the electron acceptor (3.23%). The higher PCE of the solar cell based on P3HT:CN-$PC_{70}BM$ is related to the increase in both the short circuit current (J_{sc}) and the open circuit voltage (V_{oc}). The increase in J_{sc} is related to the stronger light absorption of CN-$PC_{70}BM$ in the visible region of the solar spectrum as compared to that of $PC_{70}BM$. In other words, more excitons are generated in the bulk heterojunction (BHJ) active layer. On the other hand, the higher difference between the LUMO of CN-$PC_{70}BM$ and the HOMO of P3HT causes an enhancement in the V_{oc}. The addition of 2% (v/v) 1-chloronapthalene (CN) to the THF solvent during film deposition results in an overall improvement of the PCE up to 5.83%. This improvement in PCE can be attributed to the enhanced crystallinity of the blend (particularly of P3HT) and more balanced charge transport in the device.

1. Introduction

Organic semiconductor research for photovoltaic applications has the potential to provide clean and renewable energy sources. Organic thin-film solar cells may one day be better than traditional inorganic photovoltaic devices in terms of material and the possibility to develop large area, light, and flexible energy conversion sources by means of simple, cost-effective and environmentally friendly technologies.[1] Organic photovoltaic devices (OPVs) basically involve a heterojunction (HJ) between a donor (D) and an acceptor (A) material. Excitons resulting from light absorption by the donor (or the acceptor) diffuse to the D/A interface where they are separated into electrons and holes by the interfacial electric field. OPVs are developed in two types of architectures, namely, bilayer D/A planar heterojunctions (PHJs)[2] and bulk heterojunctions (BHJs), in which the D/A interface is distributed over the entire volume of a phase-segregated composite consisting of the two materials.[1,3] Because of the short diffusion distance of excitons in organic materials, BHJs with optimized morphologies present a much larger interfacial D/A contacting area, which thus allows the collection and dissociation of a larger number of excitons and hence improved power-conversion efficiency (PCE).

During the past ten years, BHJs based on soluble π-conjugated polymers and fullerene derivatives have been intensively investigated and their PCE has gradually increased to values of around 5.0% for cells based on poly(3-hexylthiophene) (P3HT) and phenyl-C_{60}-butyric acid methyl ester ($PC_{60}BM$),[3a–c] and to 7.0%–8.0% for devices based on low-bandgap polymers and $PC_{70}BM$.[3d–g]

However, further improvement of the PCE is limited by the high HOMO (highest occupied molecular orbital) and LUMO (lowest unoccupied molecular orbital) energy levels of P3HT and the large energy offset between the LUMO energy level of P3HT and that of $PC_{60}BM$ or $PC_{70}BM$, which results in a lower open circuit voltage (ca. 0.6 V) of the devices based

Dr. S. P. Singh, CH. P. Kumar
Inorganic & Physical Chemistry Division
CSIR-Indian Institute of Chemical Technology
Uppal road, Tarnaka, Hyderabad 500607, India
E-mail: spsingh@iict.res.in
Dr. G. D. Sharma
R & D Centre for Engineering and Science
Jaipur Engineering College
Kukas, Jaipur, Rajasthan 303101, India
E-mail: sharmagd_in@yahoo.com
Dr. R. Kurchania
Department of Physics
Maulana Azad National Institute of Technology (MANIT)
Bhopal 462051 (MP), India
Dr. M. S. Roy
Defence Laboratory, Jodhpur (Rajasthan) 342011, India

DOI: 10.1002/adfm.201200729

on P3HT/$PC_{60}BM$. To improve the PCE of polymer solar cells (PSCs), great effort has been devoted to the design and synthesis of new conjugated polymer donors[4] and new fullerene-derivative acceptor materials.[5–7] It is expected that the PCE can be enhanced, if the V_{oc} is significantly improved. It has been demonstrated that the magnitude of the V_{oc} value is proportional to the energy difference between the HOMO of the donor and the LUMO of the acceptor energy level. On the molecular level, either lowering the HOMO level of the polymer or raising the LUMO level of the fullerene material could reach greater theoretically V_{oc} values. Although extensive research effort has been directed to the development of new low-bandgap polymers by employing a donor–acceptor approach, manipulating the HOMO energy level of the D-A polymers remains challenging, because the HOMO of the polymers is not only governed by the electron-rich donor units but it is also associated with the electron-deficient acceptor units. The lowering of the HOMO level of the polymer may also inevitably increase its optical bandgap and, thereby, sacrifice its light-harvesting ability. Developing new fullerene-based materials that possess intrinsically high LUMO energy levels is a more achievable alternative to optimize the V_{oc} value. Youjun He et al. recently synthesized an indene-C_{60} bis-adductor ($IC_{60}BA$)[6a] and Li and coworkers[6b] designed a series of PCBM esters with different alkyl chain lengths of their side chain indene-C_{70} bisadduct ($IC_{70}BA$),[7] all with higher LUMO energy levels than PCBM. The higher LUMO energy levels of these fullerene derivatives led to a higher V_{oc} and improved PCE of the PSCs based on these molecules as acceptor and P3HT as donor; the PCE of a PSC based on P3HT:ICBA reached 6.5%[6a] and the PSCs based on P3HT/IC70BA showed a PCE of 5.64%.[7]

A major drawback in the synthesis of bis-adducts of fullerenes is that the formed products consist of a mixture of regioisomers that cannot easily be separated because of experimental difficulties. Chemically modified fullerenes for BHJ solar cells have been recently reviewed.[8] The synthesis of new fullerene derivatives with stronger visible absorption and higher LUMO energy levels than PCBM is currently a challenge for all those chemists engaged in the chemical modification of fullerenes for PV applications.

Recently, Mikroyannidis and coworkers reported a modified PCBM derivative F, in which the ester methyl group of PCBM was replaced by a 4-nitro-4′-hydroxy-α-cyanostilbene moiety to increase the absorption and enhance the solubility.[9] By using F as the acceptor and P3HT as the electron donor a higher performance of this solar cell was reported in comparison to PCBM-based devices. The same research group have recently used another modified PCBM, derivative A, which is a mixture of monoadduct and multiadducts, as the electron acceptor for a BHJ OPV with P3HT as the electron donor.[10] They reported a PCE of 5.32% when the P3HT:A blend was cast from mixed solvent and thermally annealed before being used as the BHJ active layer. Recently Cheng et al. have reported that BHJ OPVs based on a P3HT:di(4-methyl-phenyl)methano-C60 (DMP-PCBA) blend exhibit an open circuit voltage of 0.87 V, short circuit current of 9.05 mA cm^{-2} and a fill factor of 0.65%, leading to a high PCE of 5.2%.[11] More recently Wudl and coworkers reported a new fullerene/dispersed red denoted as PCBDR to enhance the photon absorption of fullerene derivatives in the visible region.[12]

Recently Li et al. have investigated the effect of using 3-methylthiophene (MT) and 3-hexylthiophene (HT) as a processing additive in the P3HT:$IC_{70}BA$ blend solution on the photovoltaic performance of the corresponding PSCs.[13] The PCE of the PSCs was improved from 5.80% for the device without the additive to 6.35% for the device with HT additive and to 6.69% with the MT additive.[13]

Herein, we report a new fullerene chromophore, modified $PC_{70}BM$ (**CN-PC_{70}BM**), that strongly absorbs light in the range of 350–550 nm because of the presence of a cyanovinylene 4-nitrophenyl segment (**Scheme 1**). It has been well established that the incorporation of this segment to various polymers[14] or small molecules[15] broadened their absorption spectra. Our synthesis was designed so as to maintain the major structural characteristics of $PC_{70}BM$ while introducing an extra light-absorbing moiety that is so bulky that it affects the electron transport in fullerene. The LUMO level of **CN-PC_{70}BM** is around –3.75 eV compared to –3.90 eV for $PC_{70}BM$. We have investigated the photovoltaic response of the BHJ devices based on P3HT:**CN-PC_{70}BM**, where **CN-PC_{70}BM** was used as electron acceptor, sandwiched between indium tin oxide (ITO)/poly(3,4-ethylenedioxythiophene):poly(styrenesulfonate) (PEDOT:PSS) and Al electrodes. The PSC based on the P3HT:**CN-PC_{70}BM** blend cast from THF solvent exhibited a V_{oc} of 0.82 V, J_{sc} of 10.64 mA cm^{-2}, and PCE of 4.88%, which are higher than that for devices based on P3HT:$PC_{70}BM$. We have also investigated the effect of adding CN to the THF solvent during the processing of the BHJ active layer on the PV response of PSCs and achieved a PCE of 5.83% with J_{sc} of 11.75 mA cm^{-2} and V_{oc} of 0.80 V. The enhanced crystallinity of the blend with additive leads to an increase in the hole mobility, causing a balanced charge transport, resulting in higher photocurrents.

2. Experimental Section

2.1. Materials

Acetic acid (CH_3COOH), hydrochloride (HCl), triethyl amine (Et_3N), toluene, dichloromethane (DCM), 1-hydroxy benzotriazole hydrate (HOBT.hydrate), 1-(3-dimethylamino propyl)-3-ethyl carbodimide.HCl (EDC.HCl), poly(3-hexylthiophene-2,5-diyl) (P3HT), and [6,6]-phenyl-C_{71}-butyric acid methyl ester ($PC_{70}BM$) were purchased from Sigma Aldrich and used without further purification.

2.2. Synthesis of $PC_{70}BM$ Acid

Acetic acid (30 mL) and HCl (12 mL) were added to a solution of $PC_{70}BM$ (200 mg, 0.194 mmol) in 30 mL of toluene, and the mixed solution was heated to reflux for 18 h. After the reaction the mixture was evaporated, the crude product was treated with methanol, and centrifuged to collect the suspension. This procedure was repeated with diethyl ether, toluene, and twice with diethyl ether, to yield 125 mg (63%) of $PC_{70}BM$ acid.

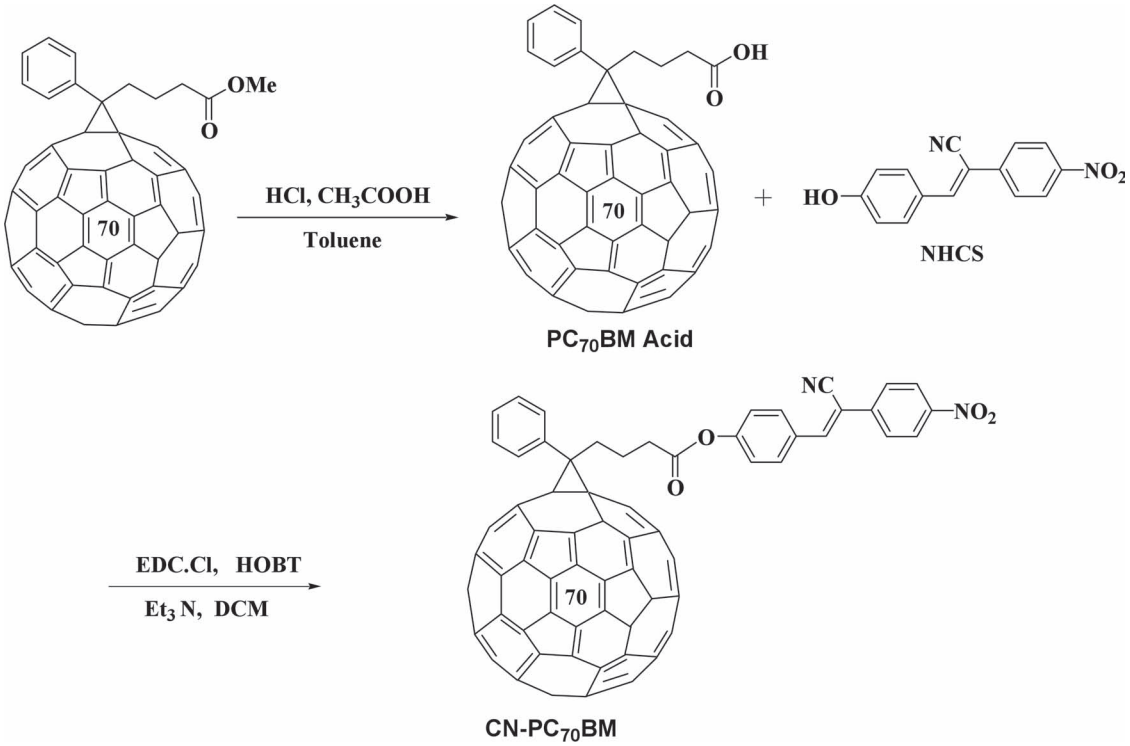

Scheme 1. Synthesis of **CN-PC_{70}BM.**

2.3. Synthesis of CN-PC_{70}BM

To a mixture of 3-(4-hydroxy phenyl)-2-(4-nitrophenyl)acrylonitrile (NHCS; 19.6 mg, 0.738 mmol), PC_{70} BM acid (50 mg, 0.0492 mmol), and NEt_3 (0.14 mL, 0.0984 mmol) in dichloromethane (DCM) (5 mL) were added l-ethyl-3-[3-(dimethylamino)propyl] carbodiimide hydrochloride (EDC.HCl) (5.65 mg, 0.0295 mmol) and 1-hydroxybenzotriazole (HOBT) (3.98 mg, 0.0295 mmol) at 0 °C. The reaction mixture was stirred at room temperature overnight and concentrated in vacuum. H_2O was added (25 mL) to the resulting residue and extracted with EtOAc. The combined organic extracts were washed with aqueous K_2CO_3 and dried over Na_2SO_4. The solvent was removed in vacuum and the residue was separated using flash chromatography (SiO_2, EtOAc) to give the expected product (yield 25 mg, 40%) of **CN-PC_{70}BM.** 1H NMR: δ 8.18 (m, 2H); 7.84–7.06 (m, 12H); 2.87 (t, 2H); 2.36 (t, 2H); 2.07 (m, 2H).

2.4. Fabrication of BHJ Solar Cells

Solar cells were fabricated on indium tin oxide (ITO)-coated glass substrates. The ITO-coated glass substrates were first cleaned with detergent, ultrasonicated in water, acetone, and isopropyl alcohol, and subsequently dried overnight in an oven. PEDOT:PSS (Baytron) was spin cast from an aqueous solution at 4000 rpm for 50 s to form a film of about 50 nm thickness. The substrate was dried at 120 °C for 10 min in air atmosphere. A solution containing a mixture of P3HT:CN-PC_{70}BM in THF or mixed solvent (1:1 w/w, 10 mg mL^{-1} for P3HT) was spin cast on top of the PEDOT:PSS films. Finally, the aluminum (Al) cathode (ca. 80 nm) was deposited through a shadow mask by thermal evaporation under a vacuum of about 3×10^{-6} Torr. The active area of the device was 15 mm^2. For thermal annealing, the blend films were placed on a hot plate and heated at 120 °C for 2 min and then cooled down to room temperature, before deposition of the Al cathode. The illuminated current–voltage (J–V) characteristics of the device were measured under AM 1.5 G filtered spectra at an incident intensity of 100 mW cm^{-2}, using a computer-controlled Keithley 238 source meter. The incident photon to current efficiency (IPCE) of the devices was recorded under illumination by a 100 W xenon lamp with a monochromator and the resulting current was measured using a Keithley electrometer under short-circuit conditions. In order to investigate the hole and electron mobilities of the different blend films unipolar devices, namely ITO/PEDOT:PSS/blend/Au (hole only) and Al/blend/Al (electron only), were prepared.

3. Results and Discussion

3.1. Optical and Electrochemical Characterization

For photovoltaic applications, the absorption in the visible region is the most significant property. For this reason PC_{70}BM is superior to PC_{60}BM when it is used as acceptor in BHJ polymer solar cells. However, PC_{70}BM also does not show much absorption in the visible region of the solar spectrum. The optical absorption spectra of PCBM, **CN-PC_{70}BM**, and P3HT are shown in **Figure 1**. The thickness of each film was about 60 nm. It can

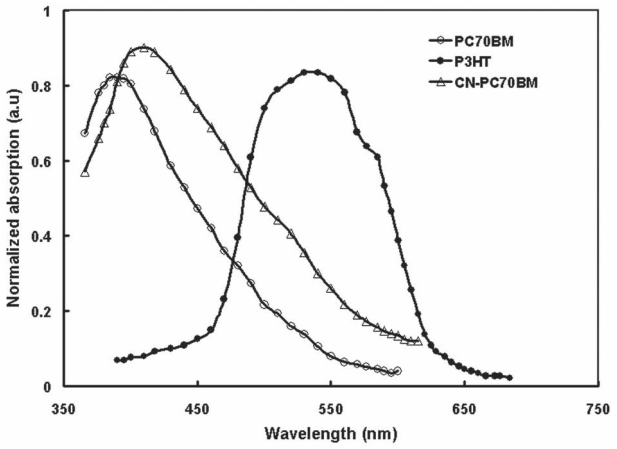

Figure 1. Optical absorption spectra of $PC_{70}BM$, **CN-$PC_{70}BM$**, and P3HT thin films cast from THF solvent.

be seen from this figure that the absorption of **CN-$PC_{70}BM$** is stronger than that of $PC_{70}BM$ in the visible region from 350 nm to 550 nm. It should be noted that certain modified fullerenes, such as an indene-C_{60} bis adduct and CN-modified $PC_{60}BM$, show stronger absorption in the visible region. The electrochemical properties of both $PC_{70}BM$ and **CN-$PC_{70}BM$** were evaluated by cyclic voltammetry. In comparison to the LUMO level of $PC_{70}BM$ (–3.9 eV), **CN-$PC_{70}BM$** showed a higher LUMO energy level, introducing the cyano and nitro group at the para-position, the LUMO level was located at –3.75 eV.

3.2. Photovoltaic Properties on BHJ Polymer Solar Cells

The current–voltage characteristics of the ITO/PEDOT:PSS/P3HT:CN-PC_{70} BM/Al devices (blend P3HT:**CN-$PC_{70}BM$** prepared under different conditions) are shown in **Figure 2** and the

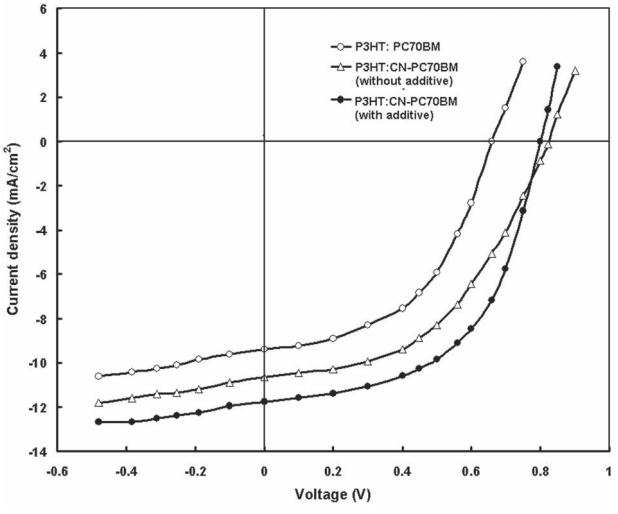

Figure 2. Current–voltage characteristics under illumination intensity (100 mW cm^{-2}) of polymer BHJ devices based on P3HT:$PC_{70}BM$ (THF cast), P3HT:**CN-$PC_{70}BM$** (THF without additive), and P3HT:**CN-$PC_{70}BM$** (with CN additive THF).

Table 1. Photovoltaic performance of PSC devices with and without additive, under the illumination intensity of AM 1.5 100 mW cm^{-2}.

Blend	J_{sc} [mA cm^{-2}]	V_{oc} [V]	FF	PCE [%]
P3HT:$PC_{70}BM$[a)]	9.40	0.66	0.52	3.23
P3HT:CN-$PC_{70}BM$[a)]	10.64	0.82	0.56	4.88
P3HT:CN-$PC_{70}BM$[b)]	11.75	0.80	0.62	5.83

[a)]Blend without CN additive; [b)]blend with CN additive.

corresponding device parameters with optimal blending ratio are compiled in **Table 1**. The photovoltaic parameters for the device based on $PC_{70}BM$ as electron acceptor are also shown for comparison. Indeed, the newly developed **CN-$PC_{70}BM$** effectively improves the V_{oc} of the device. Compared to the performance of the P3HT:$PC_{70}BM$ (1:1 w/w) based device, the device using the P3HT:**CN-$PC_{70}BM$** blend (1:1 w/w) showed both a higher J_{sc} (10.64 mA cm^{-2}) and V_{oc} (0.82 V), leading to a higher PCE of 4.88%. The higher value of the V_{oc} for the device with P3HT:**CN-$PC_{70}BM$** is attributed to the higher LUMO level of **CN-$PC_{70}BM$**, as it is well known that the V_{oc} of a BHJ polymer solar cell is proportional to the difference in the HOMO level of the donor and the LUMO level of the acceptor. The increase in J_{sc} for the device based on P3HT:**CN-$PC_{70}BM$** compared to that for P3HT:$PC_{70}BM$ can be attributed to the broader absorption band of P3HT:**CN-$PC_{70}BM$** as compared to that of its P3HT:$PC_{70}BM$ counterpart, which causes an enhancement in the light-harvesting property. This effect enhances the photogenerated excitons in the blend and leads to an improved J_{sc} and overall higher PCE.

The photovoltaic performance of PSCs can also be optimized by tuning the device fabrication conditions, such as changing the weight ratio of donor/acceptor (D/A),[17] using heat-treatment[18] or solvent annealing,[19] adding additives,[20] and using mixed solvents.[21] Among the device fabrication conditions, the simple processing by adding an additive in the blend solutions of the donor and acceptor can often improve the photovoltaic performance of the PSCs significantly. For example, Heeger and coworkers increased the PCE of a PSC based on PCPDTBT:$PC_{70}BM$ from 2.8% to 5.5% by adding 1,8-octanedithiol (OT) to the mixed solvent.[20a] Equally, 1,8-diiodooctane (DIO) is also an efficient processing additive for improving the photovoltaic performance of PSCs,[19] and 1-chloronaphthalene (CN)[20c] plays an important role in controlling the optimal morphology and creating a better interpenetrating network in Si-PDTBT:$PC_{70}BM$.[20d]

3.3. Effect of Solvent Additive

In order to improve the PCE of the P3HT:**CN-$PC_{70}BM$** based polymer solar cell, we studied the effect of additives in the THF solution on the photovoltaic performance of the devices. The optimized device fabrication conditions of our polymer solar cells were based on the P3HT:**CN-$PC_{70}BM$** blend cast from CN/THF solvent with a weight ratio of 1:1 and subsequent thermal

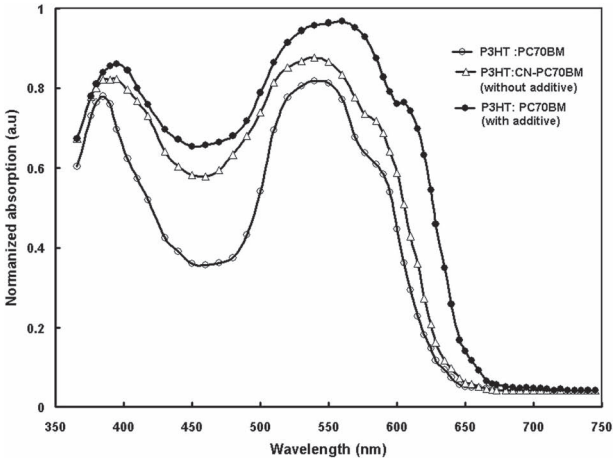

Figure 3. Optical absorption spectra of P3HT:$PC_{70}BM$ (THF cast), P3HT:**CN-$PC_{70}BM$** (without CN additive), and P3HT:**CN-$PC_{70}BM$** (with CN additive).

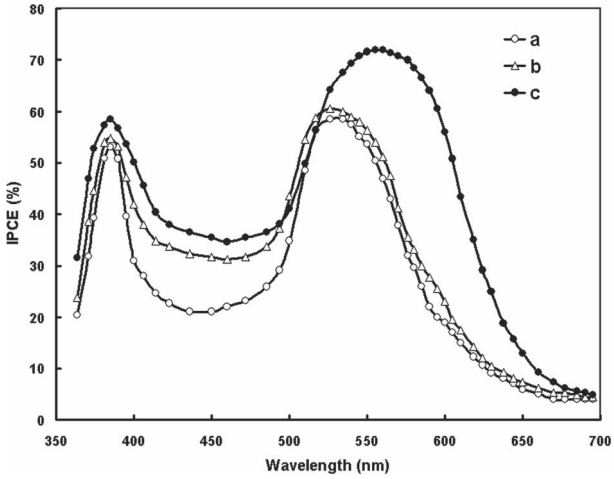

Figure 4. IPCE spectra of BHJ polymer solar cells cast from P3HT:PC70BM (a: empty circles), P3HT:**CN-$PC_{70}BM$** (cast from THF) (b: empty triangles), and P3HT:**CN-$PC_{70}BM$** (cast from CN additive THF) (c: filled circles) blends.

annealing at 120 °C for 5 min. For studying the effect of using an additive to the solvent, namely, 1-chloronaphathalene (CN), on the photovoltaic performance we used these optimized device fabrication conditions. We found that adding 2% (v/v) of CN into the THF solution of P3HT and **CN-$PC_{70}BM$** prior to spin coating, the PCE increased to 5.83%.

The *J*–*V* characteristics of the device based on the P3HT:**CN-$PC_{70}BM$** blend cast from CN/THF solution are shown in Figure 2 and the photovoltaic parameters are complied in Table 1. We can see that the photovoltaic parameters J_{sc} and FF have significantly improved (up to 11.75 mA cm^{-2} and 0.62, respectively), however, the V_{oc} decreased slightly from 0.82 V to 0.80 V, resulting in an overall PCE of 5.83%.

Figure 3 shows the optical absorption spectra of P3HT:**CN-$PC_{70}BM$** blend thin films with and without CN additive. The blend film with CN additive showed a stronger absorption band at 450–650 nm compared to that for the blend film without CN additive. In addition there is a vibronic absorption shoulder at 605 nm in the absorption spectra, belonging to the absorption of P3HT. The absorption peak at 530 nm corresponds to a π–π^* transition absorption, and the shoulder peak observed at 600–615 nm derives from the vibronic absorption of ordered P3HT crystalline regions in the film. Upon the addition of CN in the blend film, the absorption band corresponding to the P3HT is red shifted and the intensity also increased. Therefore, the red shift in the absorption band and stronger vibronic shoulder peak observed in the absorption spectra of the P3HT:**CN-$PC_{70}BM$** film with CN additive results from a more extensive P3HT crystallinity in the blend film. This indicates that adding CN into the P3HT:**CN-$PC_{70}BM$** blend solution in THF results in a higher ordered crystal structure of P3HT as compared to the film without additive.

To check the contributions from the absorptions of the donor and acceptor materials to the photocurrent, we measured the IPCE of the devices. The IPCE spectra of the devices based on the different blends are shown in **Figure 4**. It can be seen from this figure that the IPCE spectra of these devices closely resemble the absorption spectra of the blends, indicating that both components (donor and acceptors) used in the blend active layer of the device contribute to the photocurrent. The resemblance of the IPCE spectra of the devices with their optical absorption spectra also indicates the formation of a BHJ photoactive layer and increased D/A interfacial area in the device. It can be noted that the IPCE values in the wavelength region of 380–500 nm is higher for the device based on the P3HT:**CN-$PC_{70}BM$** blend than that for its P3HT:$PC_{70}BM$ counter part, which can be ascribed to the more-effective photon absorption by **CN-$PC_{70}BM$** as compared to $PC_{70}BM$. This result indicates that the **CN-$PC_{70}BM$** acceptor is more beneficial for light harvesting than $PC_{70}BM$ and results in higher J_{sc}.

The increase in the IPCE in the longer wavelength region for the device based on the P3HT:**CN-$PC_{70}BM$** blend processed with additive may be attributed to the broadening of the absorption band of the blend. The maximum J_{sc} can be estimated from the following expression

$$J_{sc} = \int_{\lambda_1}^{\lambda_2} q\,\mathrm{IPCE}(\lambda)\,N_{ph}(\lambda)\mathrm{d}\lambda \quad (1)$$

where N_{ph} (λ) is the photon flux intensity in the solar spectrum at any wavelength (λ), q is the electronic charge, and λ_1 and λ_2 are the wavelengths that correspond to the lower and upper limits of the IPCE spectra, respectively. The values of J_{sc} estimated from the above expression were 10.80 mA cm^{-2} and 12.05 mA cm^{-2} for devices based on blends processed without and with additive, respectively, which are consistent with the experimentally observed values.

In order to further investigate the effect of additive on the crystallinity of P3HT in the P3HT:**CN-$PC_{70}BM$** blend film, we measured the X-ray diffraction (XRD) patterns of the blend films prepared with and without CN additive. The thickness of the film used to record the XRD pattern was about 60 nm. We also recorded the XRD pattern of both $PC_{70}BM$ and CN-$PC_{70}BM$ as cast films and did not observe any peak from 2θ = 4 to 20°. The XRD pattern of CN-$PC_{70}BM$ in the wide span is shown in Figure S1 (Supporting Information). **Figure 5**

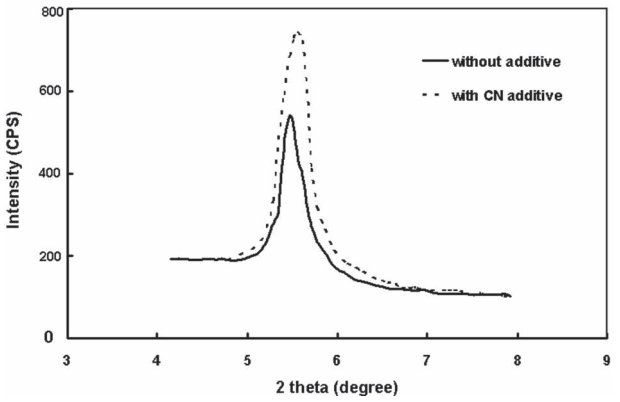

Figure 5. XRD patterns of P3HT:**CN-PC$_{70}$BM** cast from THF solution with and without CN additive.

compares the XRD pattern for the P3HT-CN-PC$_{70}$BM films prepared with and without additive in the 2θ = 4–9° range. The XRD patterns over a wider range of 2θ = 4–20° are shown in Figure S2. It can clearly be seen that the XRD peak intensity increased when the blend film was prepared from the CN additive in blend solution. Furthermore, the XRD peak of the blend film cast from the solvent with additive also shifted to a slightly higher 2θ value. The XRD peak at 2θ = 5.48° corresponds to the interlayer spacing of P3HT-ordered aggregations. The stronger XRD peak of the blend film cast from the solvent with additive indicates the increased crystallinity of P3HT, which is in agreement with the increased absorbance of the blend film as discussed above. The XRD peak of the blend film cast with additive shifted from 5.48° (interlayer spacing of 16.48 Å) to 5.56° (interlayer spacing of 16.34 Å). The reduction of the interlayer spacing in the blend film cast from the solvent with additive could be helpful for charge transportation in the corresponding device. The absorption spectra and the XRD patterns reveal that the crystallinity of P3HT was enhanced for the blends cast from solution with additive. It was observed that the FF of these devices increased from 0.56 to 0.62 only because of the additive. This indicates that the FF is not only influenced by charge-transport properties but also by interface contacts between the active layer and the electrodes.[22]

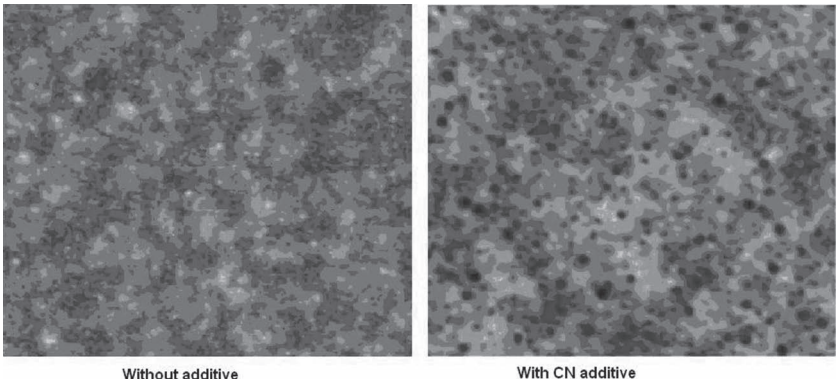

Figure 6. AFM images of P3HT:**CN-PC$_{70}$BM** blend thin films cast from THF solution with and without CN additive.

The morphology and interpenetrating network of the blend used for the fabrication of BHJ polymer solar cells are very important factors that influence the performance. Therefore, we have measured the morphology of P3HT:**CN-PC$_{70}$BM** blend films prepared with and without CN additive by atomic force microscopy (AFM). **Figure 6** shows the AFM images of the blend films. From these AFM images the root mean square surface roughness values are about 12.6 nm and 10.8 nm for the films cast with and without CN additives, respectively. The films cast from solution with additive have thus a rougher surface which could be beneficial to a higher photovoltaic performance of the corresponding PSCs as in the case of P3HT:PC$_{70}$BM based device.[13] The rough surface and finer interpenetrating network of the active layer for the device with additive may result from a better nanoscaled phase separation between the crystalline P3HT donor and **CN-PC$_{70}$BM** acceptor. The finer interpenetrating networks between the P3HT donor and **CN-PC$_{70}$BM** acceptor increase the D-A interfaces for exciton dissociation, resulting in an improvement in the J_{sc} and PCE of the corresponding device.

For efficient polymer solar cells the mobilities of electrons and holes in the BHJ active layer are important parameters and must be well balanced for efficient charge transport and are an essential prerequisite for increasing the PCE. The electron and hole mobilities of the P3HT:**CN-PC$_{70}$BM** blend films were estimated using electron- and hole-only devices prepared from the blends cast from THF with and without CN additive, using space charge limited current (SCLC) theory. The *J*–*V* characteristics were fitted according to:[16]

$$J_{SCLC} = (9/8)\varepsilon\mu\left(\frac{V^2}{L^3}\right) \quad (2)$$

where ε is the permittivity of the blend film, μ is the charge carrier (electron or hole) mobility, L is the film thickness, and V is the applied field. **Figure 7** shows the variation of dark current of an ITO/PEDOT:PSS/P3HT:**CN-PC$_{70}$BM**/Au hole-only device with corrected bias voltage, which is determined by the difference in the work function of Au and the HOMO level of PEDOT:PSS. In the trap-free SCLC region, where all the traps are filled, the SCLC behavior can be characterized by the Mott–Gurnay square law as described above. Similar characteristics have been observed for Al/P3HT:**CN-PC$_{70}$BM**/Al electron-only devices. The hole and electron mobilities were estimated by fitting the experimental data with Equation 2. The hole mobilities for the blend films processed with and without additive were 4.67×10^{-6} cm^2 V^{-1}s^{-1} and 1.6×10^{-4} cm^2 V^{-1}s^{-1}, respectively. The electron mobilities for the blend films processed with and without additive were 1.8×10^{-4} cm^2 V^{-1}s^{-1} and 4.65×10^{-4} cm^2 V^{-1}s^{-1}, respectively. Both the hole and electron mobilities for the blend films processed with additive are higher than those for the films cast without additive. The hole mobility improved by two orders of magnitude but the electron mobility increased only by a factor of 2.5. The increase in hole mobility can be attributed to

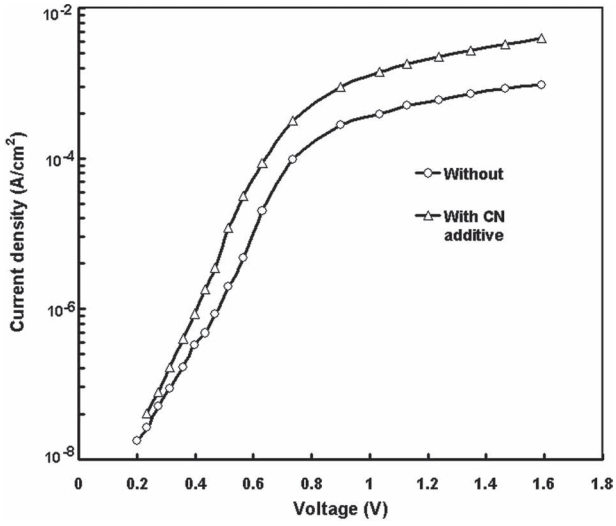

Figure 7. Dark current–voltage characteristics of ITO/PEDOT:PSS/P3HT:**CN-PC$_{70}$BM**/Au cast from THF solution with and without CN additive.

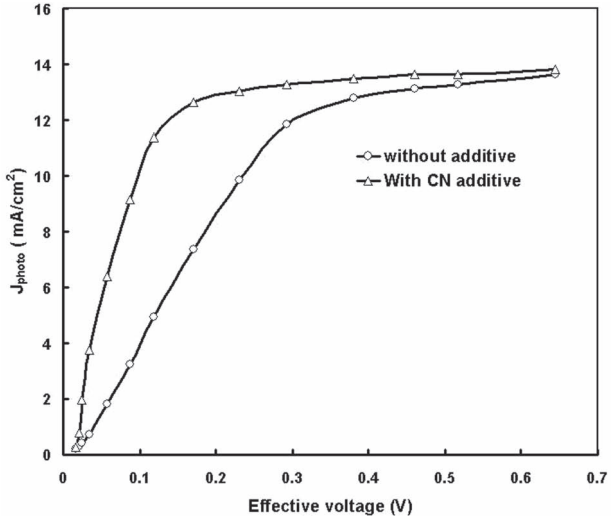

Figure 8. Variation of photocurrent $J_{photo} = J_{light}–J_{dark}$) as a function of effective applied voltage (V_0–V_{app}) for BHJ polymer solar cells cast from THF solution with and without CN additive.

the increased crystalline nature of P3HT in the blend as indicated by the absorption spectra and XRD data. The ratio of electron and hole mobilities for the blend cast from solution with and without additive were 38.5 and 2.9, respectively, indicating a more balanced charge transport in the device based on the P3HT:**CN-PC$_{70}$BM** blend processed with additive. If the charge transport in the device is unbalanced (blend cast from THF, where the mobility ratio is high), hole accumulation occurs in the device and the photocurrent is space-charge limited.[23] The smaller value of mobility ratio indicates a more balanced charge transport that reduces the space-charge effect and results in an improvement in the J_{sc} and overall PCE.

The exciton dissociation efficiency in the BHJ is also an important factor affecting the PCE of the BHJ solar cell. The generation rate of the fee carriers (G) can be described by

$$G(T,E) = G_{max}\, P(T,E) \quad (3)$$

where G_{max} is the maximum generation rate of bound electron–hole pairs, $P(T,E)$ is the probability of charge separation at the donor–acceptor interface,[24] limited by the temperature (T) and the electric field (E). As the photocurrent is determined by the rate of generation of free carriers, which is governed by the probability of charge separation, and the exciton dissociation efficiency, similar to the probability of charge separation, is also an important process for enhancing the device performance. Therefore, the $P(T,E)$ of devices based on blends processed with and without additive was compared to obtain information on changes in J_{sc}. In reverse bias mode, the photocurrent is often plotted as a function of the effective applied voltage. The photocurrent is then defined as $J_{photo} = J_{light}–J_{dark}$, where J_{light} and J_{dark} are the current densities of the device measured under illumination and in the dark, respectively. The effective voltage is then defined as $V_{eff} = V_0–V_{appl}$, whereby V_0 is the compensation voltage defined as the voltage for $J_{photo} = 0$, and V_{appl} is the applied voltage. **Figure 8** shows a log–log plot of J_{photo} arising from the J–V curves of P3HT:**CN-PC$_{70}$BM** based devices processed from solution with and without additive as a function of V_{eff}. The photocurrent increases linearly in the low-voltage region and subsequently tends to saturate in the higher voltage region. The photocurrent could be estimated by $J_{photo} = qG(T,E)d$ in the saturation region for $V_{eff} > 0.3$–0.4 V. In the high-voltage region (>0.8 V), most of the bound electron–hole pairs were separated, thus $J_{sat} = qG_{max}d$. Under short-circuit conditions, the value of J_{sc}/J_{sat} gives information about the charge-separation efficiency. This value is 0.95 and 0.82 for the devices based on blend films processed with and without additive, respectively. Recombination is also an important process in charge-separation efficiency and has a strong influence on the charge collection. It has been reported that if $J_{sc}/J_{sat} > 0.9$ charge extraction is much more efficient than charge recombination.[25] The value of J_{sc}/J_{sat} for the device with CN additive was 0.95 indicating that the charge-extraction process is more efficient than recombination in these devices.

The photocurrent in BHJ polymer solar cells is determined by the product of absorbed photons within the solar spectrum and the incident photon to current efficiency (IPCE). It can be seen from the absorption spectra of the blends that the absorption band is broadened if the blend is processed with additive and its intensity also improved. This reveals that the number of photons absorbed by the blend processed with additive is higher than that of blends processed without additive. Therefore the higher value of J_{sc} may be related to this effect. The IPCE is determined by three processes: i) migration and diffusion of photogenerated excitons towards the D/A interface, ii) exciton dissociation into free electrons and holes at the D/A interface, and iii) collection of electrons and holes by cathode and anode, respectively. Process (i) depends on the nanoscale phase separation between the donor and acceptor used in the blend active layer. Process (ii) depends on the difference between the LUMO levels of the donor and acceptor materials used in the blend and the interfacial area of the D-A interface. Process (iii) is related to the mobilities of the charge carriers and the ratio of these mobilities.

As discussed above, the higher value of the rms roughness and better interpenetrating networks for the blend processed with additive leads to increased D-A interfacial area, and, thus, to more efficient exciton dissociation. The enhancement in the hole mobility and more balanced ratio between the electron and hole mobilities results in more efficient charge collection. These combined effects result in an enhancement in the overall PCE of the device based on the blend processed with additive.

4. Conclusions

A modified $PC_{70}BM$, namely **CN-PC_{70}BM**, which contains a cyanovinylene 4-nitrophenyl segment, was synthesized and showed a much stronger absorption in the visible region as compared to $PC_{70}BM$. We have fabricated PSCs with the P3HT:**CN-PC_{70}BM** blend sandwiched between ITO/PEDOT:PSS and Al electrodes. The V_{oc} and J_{sc} values of the BHJ PSC based on the P3HT:**CN-PC_{70}BM** blend cast from THF solution reached 0.82 V and 10.64 mA cm^{-2}, respectively, leading to an overall PCE of 4.88%, which is significantly improved compared to devices based on P3HT:$PC_{70}BM$ (PCE = 3.23%). The increase in J_{sc} could be attributed to the stronger absorption of **CN-PC_{70}BM** in the visible region as compared to $PC_{70}BM$. However, the increase in V_{oc} was ascribed to the higher LUMO level of **CN-PC_{70}BM** compared to that of $PC_{70}BM$. We have also investigated the effect of adding CN during processing of the P3HT:**CN-PC_{70}BM** blend from THF solution on the photovoltaic performance of the corresponding PSC. The PCE was improved from 4.88% for the device without additive to 5.83% for the device with CN additive. The results of optical absorption spectroscopy, XRD analysis, and AFM measurements all show that the active layer of the P3HT:**CN-PC_{70}BM** blend cast from THF solution with CN additive has strengthened absorbance, enhanced crystallinity, and improved film morphology, which leads to enhanced charge transport and improved overall PCE.

Supporting Information

Supporting Information is available from the Wiley Online Library or from the author.

Acknowledgements

The authors are thankful to Dr. J. S. Yadav, Director of IICT and Dr. M. Lakshmi Kantam, HOD, I&PC Division for their constant encouragement. The authors are also thankful to Dr. V. Jayathirtha Rao for helpful discussions. This work was supported by the CSIR-IICT-NWP-54. Ch. P.K. thanks UGC, New Delhi for a junior research fellowship. This article was modified on October 10, 2012 to correct an error in Scheme 1 that was present in the version originally published online.

Received: March 15, 2012
Revised: April 20, 2012
Published online: June 12, 2012

[1] a) S. Gunes, H. Neugebauer, N. S. Sariciftci, *Chem. Rev.* **2007**, *107*, 1324; b) B. C. Thompson, J. M. J. Fréchet, *Angew. Chem. Int. Ed.* **2008**, *47*, 58; c) G. Denler, M. C. Scharber, C. J. Brabec, *Adv. Mater.* **2009**, *21*, 1323; d) R. Po, M. Maggini, N. Camaioni, *J. Phys. Chem. C.* **2010**, *114*, 695; e) P. Sonar, J. P. F. Li, K. L. Chan, *Energy Environ. Sci.* **2011**, *4*, 1558.

[2] a) C. W. Tang, *Appl. Phys. Lett.* **1986**, *48*, 183; b) D. Wöhrle, D. Meissner, *Adv. Mater.* **1991**, *3*, 129; c) P. Peumans, A. Yakimov, S. R. Forrest, *J. Appl. Phys.* **2003**, *93*, 3693; d) M. Riede, T. Mueller, W. Tress, R. Schueppel, K. Leo, *Nanotechnology* **2008**, *18*, 424001; e) R. de Bettignies, Y. Nicolas, P. Blanchard, E. Levillain, J.-M. Nunzi, J. Roncali, *Adv. Mater* **2003**, *15*, 1939; f) C. Ulrich, R. Schueppel, A. Petrich, M. Pfeiffer, K. Leo, E. P. Kilickiran, P. Bäuerle, *Adv. Funct. Mater* **2007**, *17*, 2991; g) R. Fitzner, E. Reinold, A. Mishra, E. Mena-Osteritz, H. Ziehkle, C. Korner, K. Leo, M. Riede, M. Weil, O. Tsaryova, A. Weiss, C. Ulrich, M. Pfeiffer, P. Bäuerle, *Adv. Funct. Mater* **2011**, *27*, 897; h) S. Steinberger, A. Mishra, E. Reinold, C. M. Müller, C. Ulrich, M. Pfeiffer, P. Bäuerle, *Org. Lett* **2011**, *13*, 90.

[3] a) G. Li, V. Shrotriya, J. Huang, Y. Yao, T. Moriarty, K. Emery, Y. Yang, *Nat. Mater.* **2005**, *4*, 864; b) W. Ma, C. Yang, X. Gong, K. Lee, A. J. Heeger, *Adv. Funct. Mater.* **2005**, *15*, 1617; c) M. Reyes-Reyes, K. Kim, D. L. Carroll, *Appl. Phys. Lett.* **2005**, *87*, 083506; d) K. Kim, J. Liu, M. A. G. Namboothiry, D. L. Carroll, *Appl. Phys. Lett.* **2007**, *90*, 163511; e) S. H. Park, A. Roy, S. Beaupre, S. Cho, N. Coates, J. S. Moon, D. Moses, M. Leclerc, K. Lee, A. J. Heeger, *Nat. Photon.* **2009**, *3*, 297; f) L. L. Liang, Z. Xu, J. B. Xia, S. T. Tsai, Y. Wu, G. Li, C. Ray, L. P. Yu, *Adv. Mater.* **2010**, *22*, E135; g) H. Zhou, L. Yang, A. C. Stuart, S. C. Price, S. Liu, W. You, *Angew. Chem. Int. Ed.* **2011**, *50*, 2995.

[4] a) J. W. Chen, Y. Cao, *Acc. Chem. Res.* **2009**, *42*, 1709; b) Y.-J. Chen, S.-H. Yang, C.-S. Hsu, *Chem. Rev.* **2009**, *109*, 5868.

[5] Y. J. He, Y. F. Li, *Phys. Chem. Chem. Phys.* **2011**, *13*, 1970.

[6] a) Y. J. He, H.-Y. Chen, J. H. Hou, Y. F. Li, *J. Am. Chem. Soc.* **2010**, *132*, 1377; b) G. J. Zhao, Y. J. He, Y. F. Li, *Adv. Mater.* **2010**, *22*, 4355.

[7] Y. J. He, G. J. Zhao, B. Peng, Y. F. Li, *Adv. Funct. Mater.* **2010**, *20* 3383.

[8] J. L. Delgado, P.-A. Bouit, S. Filippone, M. Á. Herranza, N. Martín, *Chem. Commun.* **2010**, *46*, 4853.

[9] J. A. Mikroyannidis, A. N. Kabanakis, S. S. Sharma, G. D. Sharma, *Adv. Funct. Mater* **2011**, *21*, 746.

[10] J. A. Mikroyannidis, D. V. Tasgkournos, S. S. Sharma, G. D. Sharma, *J. Phys. Chem. C* **2011**, *115*, 7806.

[11] Y. J. Cheng, M. H. Liao, C. Y. Chang, W. S. Kao, C. E. Wu, C. S. Hsu, *Chem. Mater.* **2011**, *23*, 4056.

[12] M. Wang, E. Chesnut, Y. Sun, M. Tong, M. Guide, Y. Zhang, N. D. Treat, A. Varotto, A. Mayer, M. L. Chabinyc, T. Q. Nguyen, F. Wudl, *J. Phys. Chem. C* **2012**, *116*, 1313.

[13] Y. Sun, C. Cui, H. Wang, Y. Li, *Adv. Energy Mater.* **2011**, *1*, 1058.

[14] a) J. A. Mikroyannidis, A. N. Kabanakis, P. Balraju, P. Suresh, G. D. Sharma, *Macromolecules* **2010**, *43*, 5544; b) J. A. Mikroyannidis, S. S. Sharma, Y. K. Vijay, G. D. Sharma, *ACS Appl. Mater. Interfaces* **2010**, *2*, 270.

[15] a) J. A. Mikroyannidis, M. M. Stylianakis, P. Suresh, P. Balraju, G. D. Sharma, *Org. Electron.* **2009**, *10*, 1320; b) J. A. Mikroyannidis, P. Suresh, G. D. Sharma, *Org. Electron.* **2010**, *11*, 311.

[16] A. M. Goodman, A. Rose, *J. Appl. Phys.* **1971**, *41*, 2823.

[17] J. Peet, M. L. Senatore, A. J. Heeger, G. C. Baza, *Adv. Mater.* **2009**, *21*, 1521.

[18] a) J. Huang, G. Li, Y. Yang, *Appl. Phys. Lett.* **2005**, *87*, 112 105; b) G. Li, V. Shrotriya, Y. Yao, Y. Yang, *J. Appl. Phys.* **2005**, *98*, 043704.

[19] G. Li, Y. Yao, H. Yang, V. Shrotriya, G. Yang, Y. Yang, *Adv. Funct. Mater.* **2007**, *17*, 1636.

[20] a) J. Peet, J. Y. Kim, N. E. Coates, W. L. Ma, D. Moses, A. J. Heeger, G. C. Bazan, *Nat. Mater.* **2007**, *6*, 497; b) J. K. Lee, W. L. Ma, C. J. Brabec, J. Yuen, J. S. Moon, J. Y. Kim, K. Lee, G. C. Bazan, A. J. Heeger, *J. Am. Chem. Soc.* **2008**, *130*, 3619; c) H. Y. Chen, H. Yang, G. Yang, S. Sista, R. Zadoyan, G. Li, Y. Yang, *J. Phys. Chem.*

C **2009**, *113*, 7946; d) J. S. Moon, C. J. Takacs, S. Cho, R. C. Coffin, H. Kim, G. C. Bazan, A. J. Heeger, *Nano Lett.* **2010**, *10*, 4005; e) T. Salim, L. H. Wong, B. Bräuer, R. Kukreja, Y. L. Foo, Z. Bao, Y. M. Lam, *J. Mater. Chem.* **2011**, *21*, 242.

[21] F. L. Zhang, K. G. Jespersen, C. Björström, M. Svensson, M. R. Andersson, K. Magnusson, E. Moons, A. Yartsev, O. Inganäs, *Adv. Funct. Mater.* **2006**, *16*, 667.

[22] L. M. Chen, Z. Xu, Z. R. Hong, Y. Yang, *J. Mater. Chem.* **2010**, *20*, 2575.

[23] A. J. Moule, K. Meerholz, *Adv. Mater.* **2008**, *20*, 240.

[24] a) L. J. A. Koster, E. C. P. Smits, V. D. Mihailetchi, P. W. M. Blom, *Phys. Rev. B* **2005**, *72*, 085205; b) J. H. Park, J. S. Kim, J. H. Lee, W. H. Lee, K. Cho, *J. Phys. Chem. C* **2009**, *40*, 17579.

[25] J. S. Kim, J. H. Lee, J. H. Park, C. Shim, M. Sim, K. Cho, *Adv. Funct. Mater.* **2011**, *21*, 480.